

# Semidefinite Programming Relaxation Based Virtually Antipodal Detection for Gray Coded 16-QAM MIMO Signalling

Shaoshi Yang<sup>†\*</sup>, Lajos Hanzo<sup>†</sup>, *Fellow, IEEE*

<sup>†</sup>School of Electronics and Computer Science, University of Southampton, SO17 1BJ, UK

\*School of Information and Communication Engineering, Beijing University of Posts and Telecommunications, 100876, Beijing, China

Email: {sy7g09, lh}@ecs.soton.ac.uk, http://www-mobile.ecs.soton.ac.uk

**Abstract**—An efficient semidefinite programming relaxation (SDPR) based virtually antipodal (VA) detection approach is proposed for Gray coded 16-QAM signalling over multiple-input–multiple-output (MIMO) channels. The existing index-bit-based VA-SDPR (IVA-SDPR) method is incapable of making direct binary decisions concerning the individual information bits without making symbol decisions first, except for the linear natural-mapping aided rectangular QAM constellations. By contrast, our new method is capable of directly deciding on the information bits of the ubiquitous Gray-mapping aided 16-QAM by employing a strikingly simple linear matrix representation (LMR) of 4-QAM. As an appealing benefit, the conventional “signal-to-symbol-to-bits” decision process is substituted by a simpler “signal-to-bits” decision process for the classic Gray-mapping aided rectangular 16-QAM. Furthermore, when combined with low-complexity bit-flipping based “hill climbing”, the proposed direct-bit-based VA-SDPR (DVA-SDPR) detector achieves the best bit-error-ratio (BER) performance among the known SDPR-based MIMO detectors in the context considered, while still maintaining a worst-case complexity order as low as  $O[(4N_T + 1)^{3.5}]$ .

**Index Terms**—Binary constrained quadratic programming, Gray mapping, primal-dual interior-point algorithm, QAM, semidefinite programming relaxation (SDPR), virtually-antipodal detection.

## I. INTRODUCTION

THE tree-search based sphere decoder (SD) [1], [2] derived for multiple-input–multiple-output (MIMO) channels is probably the best-known computationally efficient algorithm capable of achieving the exact maximum-likelihood (ML) performance. However, the SD is only efficient for relatively high signal-to-noise ratios (SNR) and a low number of transmit antennas  $N_T$ . Furthermore, it has an exponentially increasing *expected complexity order* of  $O(M^{\beta N_T})$  in both the worst-case and the average-case, where  $M$  is the constellation size, and  $\beta \in (0, 1]$  is a small factor depending on the value of SNR [3].

In contrast to the classic tree-search philosophy, the semidefinite programming [4] relaxation (SDPR) approach is based on convex optimization theory [5] and has recently received much research attention [6]–[12]. The most attractive characteristic of the SDPR-aided detectors is that they guarantee a so-called polynomial-time<sup>1</sup> worst-case computational complexity, while achieving a high performance. The numerical and analytical results of [6] confirmed that the SDPR detector achieves the maximum possible diversity order, when using binary phase shift keying (BPSK) for transmission over a real-valued fading MIMO channel. The SDPR approach was also further developed for high-order modulation schemes, such as for  $M$ -ary phase shift keying ( $M$ -PSK) scenario in [7], and for high-order quadrature amplitude modulation (QAM) in [8]–[11]. As for the 16-QAM scenario, it was recently shown in [12] that the so-called polynomial-inspired SDPR (PI-SDPR) [8], the bound-constrained SDPR (BC-SDPR) [9] and the virtually antipodal SDPR (VA-SDPR) [11] are actually equivalent in the sense that they attain the same optimal objective values and exhibit an identical symbol error ratio

The financial support of the China Scholarship Council (CSC), the EPSRC, UK under the auspices of the China-UK Science Bridge and that of the RC-UK under the India-UK Advanced Technology Centre is gratefully acknowledged.

<sup>1</sup>The computational complexity increases as a polynomial function of  $N_T$ .

(SER) performance<sup>2</sup>.

The VA-SDPR detector is of particular interest to us, since it may be shown to have a strong connection to the SDPR detector used in BPSK, where the SDPR shows near-optimal performance. The VA-SDPR converts the  $M$ -ary integer programming problem into a binary integer programming problem. However, in the VA-SDPR detector of [11] the binary decisions are made on the “index bits” rather than on the “information bits”. These two types of bits are in general different [11] from each other, except for the linear natural-mapping<sup>3</sup> aided rectangular  $M$ -QAM [13]. Consequently, when the ubiquitous Gray-mapping aided rectangular  $M$ -QAM is used, in order to make correct decisions on the information bits, the VA-SDPR detector of [11] has to obtain its symbol decisions based on the decided “index bits”. As shown in [13], the Gray-mapping of high-order rectangular QAM is nonlinear for  $M > 4$  and the relationship between the transmitted symbol vector and the information bits *cannot* be characterized by a compact linear matrix transformation of the form  $s = \mathbf{W}b$  as for the linear natural-mapping aided rectangular QAM, where  $s$  is the transmitted symbol vector,  $b$  is the associated antipodal information bit vector, and  $\mathbf{W}$  is the constellation-specific modulation matrix known to both the transmitter and receiver.

In this paper, we propose a novel direct-bit-based VA-SDPR (DVA-SDPR) detector for the ubiquitous Gray-mapping aided rectangular 16-QAM, which is capable of directly deciding on the information bits for transmission over fading MIMO channels. By exploiting the specific structure of the Gray-mapping aided 16-QAM constellation, our approach transforms the original 16-QAM aided  $(N_T \times N_R)$ -element MIMO system to a virtual 4-QAM aided  $(2N_T \times N_R)$ -element MIMO system. Since the modulation matrix of 4-QAM is identical for both the natural-mapping and the Gray-mapping [13], the proposed DVA-SDPR detector finally converts the classic nonlinear Gray-mapping aided 16-QAM symbol detection problem to a Boolean quadratic programming (BQP) problem [5]. When relying on this technique, the conventional “signal-to-symbol-to-bits” decision process is substituted by a simpler “signal-to-bits” decision process for the classic nonlinear Gray-mapping aided rectangular 16-QAM. In other words, we can directly carry out the information-bit decisions without invoking first conventional symbol decisions for the nonlinear Gray-mapping aided rectangular 16-QAM scheme. Furthermore, when combined with low-complexity bit-flipping based “hill climbing”, the DVA-SDPR detector achieves the best bit-error-ratio (BER) performance among the known SDPR-based MIMO detectors in the context considered, while still maintaining a polynomial-time worst-case complexity order as low as  $O[(4N_T + 1)^{3.5}]$ .

## II. SYSTEM MODEL AND PROBLEM STATEMENT

Consider a perfectly symbol-synchronized memoryless spatial multiplexing MIMO system having  $N_T$  transmit and  $N_R$  receive

<sup>2</sup>The SDPR QAM detector of [10] exhibits a better performance than that of [8], [9], [11], but has a much higher complexity.

<sup>3</sup>The linear natural mapping is defined as the mapping which satisfies eq.(3) of [13].

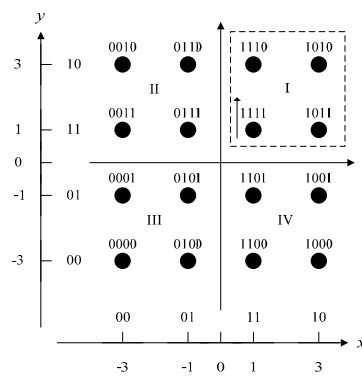


Fig. 1. Signal space diagram of the Gray-mapping aided 16-QAM.

antennas. The baseband equivalent system model is written as

$$\mathbf{y} = \mathbf{H}\mathbf{s} + \mathbf{n}, \quad (1)$$

where  $\mathbf{y}$  is the  $N_R$ -element received signal vector,  $\mathbf{s}$  is the  $N_T$ -element transmitted symbol vector, whose elements are from the Gray-coded rectangular 16-QAM constellation shown in Fig. 1,  $\mathbf{H}$  is the  $(N_R \times N_T)$ -element complex-valued channel matrix, and  $\mathbf{n}$  is the  $N_R$ -element complex Gaussian noise vector with a zero mean and covariance matrix of  $2\sigma^2\mathbf{I}$ .

The ML detection conceived for the MIMO system of (1) can be formulated as the following constrained discrete least-squares optimization problem

$$\hat{\mathbf{s}}_{\text{ML}} = \arg \min_{\mathbf{s} \in \mathbb{D}} \|\mathbf{y} - \mathbf{H}\mathbf{s}\|_2^2, \quad (2)$$

where the alphabet set  $\mathbb{D}$  represents the Gray-mapping aided rectangular 16-QAM constellation of Fig. 1.

In [11], (2) was further formulated as<sup>4</sup>

$$\hat{\mathbf{d}}_{\text{ML}} = \arg \min_{\mathbf{d} \in \{+1, -1\}^{4N_T}} \|\tilde{\mathbf{y}} - \tilde{\mathbf{H}}\mathbf{T}\mathbf{d}\|_2^2, \quad (3)$$

where  $\mathbf{d}$  represents the vector of “index bits” [11]<sup>5</sup>, which are different from the (antipodal) information-bit vector  $\mathbf{b}$ .  $\tilde{\mathbf{H}}$  and  $\tilde{\mathbf{y}}$  are the real-valued versions of  $\mathbf{H}$  and  $\mathbf{y}$  in (2) respectively, while  $\mathbf{T}$  is the real-valued transformation matrix, which is fixed for a specific constellation, similar to the complex-valued modulation matrix  $\mathbf{W}$  of [13]. After obtaining  $\hat{\mathbf{d}}_{\text{ML}}$ , the original real-valued symbol vector corresponding to the real-valued system model is estimated as

$$\hat{\mathbf{s}}_{\text{ML}} = \mathbf{T}\hat{\mathbf{d}}_{\text{ML}}. \quad (4)$$

In contrast to this solution, the problem of interest to us is — how can we develop a VA-SDPR detector that directly estimates the (antipodal) information bit vector  $\mathbf{b}$  without estimating the symbol vector  $\mathbf{s}$ ?

### III. STRUCTURE OF GRAY-MAPPING AIDED 16-QAM

Assume that the  $j$ th component of the transmitted 16-QAM symbol vector  $\mathbf{s}$  is obtained using the bit-to-symbol mapping function  $s_j = \text{map}(\mathbf{u}_j)$ ,  $j = 1, 2, \dots, N_T$ , where  $\mathbf{u}_j = [u_{j,1}, u_{j,2}, u_{j,3}, u_{j,4}]^T$  is the vector of information bits with each element being 1 or 0. The vector of information bits corresponding to  $\mathbf{s}$  is denoted as  $\mathbf{u}$ , which satisfies  $\mathbf{s} = \text{map}(\mathbf{u})$  and is formed by concatenating the  $N_T$  antennas’ information bits  $\mathbf{u}_1, \mathbf{u}_2, \dots, \mathbf{u}_{N_T}$ , yielding

<sup>4</sup>The real-valued model is used in [11], whereas we use the more general complex-valued model here.

<sup>5</sup>In general, the (real-valued) Gray-coded QAM symbol vector  $\tilde{\mathbf{s}}$  cannot be represented as a linear transformation of  $\tilde{\mathbf{s}} = \mathbf{T}\mathbf{b}$ , as shown in [13]. However, it was formulated as  $\tilde{\mathbf{s}} = \mathbf{T}\mathbf{d}$  in [11], where  $\mathbf{d}$  was termed as “index bits”.

$\mathbf{u} = [u_1, u_2, \dots, u_k, \dots, u_{4N_T}]^T = [\mathbf{u}_1^T, \mathbf{u}_2^T, \dots, \mathbf{u}_{N_T}^T]^T \in \{1, 0\}^{4N_T}$ . The antipodal information bits are obtained from the original information bits of logical 1 or 0 using  $b_k = 2u_k - 1$ , where  $b_k \in \{+1, -1\}$ .

As shown in [13], the nonlinear Gray-mapping aided 16-QAM scheme may be formulated as  $\mathbf{s} = \mathbf{W}(\mathbf{b})\mathbf{b}$ , where the structure of the modulation matrix  $\mathbf{W}(\mathbf{b})$  exhibits multiple forms, depending on the antipodal information bit vector  $\mathbf{b}$ . Hence  $\mathbf{W}(\mathbf{b})$  is not readily available at the receiver side. Although it may be possible to estimate the modulation matrix  $\mathbf{W}(\mathbf{b})$  at the receiver, the estimation error will inevitably degrade the achievable performance.

Let us revisit the “generating units” of the Gray-mapping aided 16-QAM scheme shown in Table I [13]. Since the four constellation points in the same quadrant share the same generating units, without loss of generality, we will consider the constellation points in Quadrant IV of Fig. 1 as an example.

The legitimate original information-bit-sequences  $[u_1 u_2 u_3 u_4]$  are:

$$[1 \ 1 \ 0 \ 0] \quad [1 \ 0 \ 0 \ 0] \quad [1 \ 0 \ 0 \ 1] \quad [1 \ 1 \ 0 \ 1]. \quad (5)$$

The above-mentioned generating units  $[g_1 g_2 g_3 g_4]$  corresponding to  $[u_1 u_2 u_3 u_4]$  are:

$$[2 \ -1 \ 2i \ i] \quad [2 \ -1 \ 2i \ i] \quad [2 \ -1 \ 2i \ i] \quad [2 \ -1 \ 2i \ i]. \quad (6)$$

Observing (5) and (6), two remarks can be made. Firstly, the bits  $u_1$  and  $u_3$  of the four information-bit-sequences that are mapped to the specific constellation points dwelling in the same quadrant are identical. Secondly, the first and the third components of the generating units are  $[g_1 g_3] = [2 \ 2i]$ , which indicates that the bits  $u_1$  and  $u_3$  of each information-bit-sequence are mapped to a 4-QAM constellation, whose amplitude is doubled<sup>6</sup>. Therefore, the Gray-mapping aided 16-QAM symbols of Quadrant IV can be formulated as

$$\begin{aligned} s &= \text{map}_{16\text{-QAM}}(u_1 u_2 u_3 u_4) \\ &= 2 \times \text{map}_{4\text{-QAM}}(u_1 u_3) + \text{map}_x(u_2 u_4) \\ &= 2s^{(1)} + s^{(2)}. \end{aligned} \quad (7)$$

To elucidate the notation of  $\text{map}_x(u_2 u_4)$  further, let us observe

$$[u_2 u_4] : \quad [1 \ 0] \quad [0 \ 0] \quad [0 \ 1] \quad [1 \ 1], \quad (8)$$

$$[g_2 g_4] : \quad [-1 \ i] \quad [-1 \ i] \quad [-1 \ i] \quad [-1 \ i], \quad (9)$$

$$s^{(2)} : \quad -1 - i \quad 1 - i \quad 1 + i \quad -1 + i, \quad (10)$$

where we have  $s^{(2)} = (2[u_2 u_4] - 1) \times [g_2 g_4]^T$ . Note that  $s^{(2)}$  may also be obtained by mapping the bits

$$[\tilde{u}_2 \tilde{u}_4] : \quad [0 \ 0] \quad [1 \ 0] \quad [1 \ 1] \quad [0 \ 1] \quad (11)$$

to 4-QAM, where  $s^{(2)} = (2[\tilde{u}_2 \tilde{u}_4] - 1) \times [1 \ i]^T$ .

Therefore, (7) may be reformulated as

$$s = 2 \times \text{map}_{4\text{-QAM}}(u_1 u_3) + \text{map}_{4\text{-QAM}}(\tilde{u}_2 \tilde{u}_4). \quad (12)$$

On the other hand, we have

$$\begin{aligned} 00 &= (\underline{1} \oplus 1)(\underline{0} \oplus 0), \\ 10 &= (\underline{0} \oplus 1)(\underline{0} \oplus 0), \\ 11 &= (\underline{0} \oplus 1)(\underline{1} \oplus 0), \\ 01 &= (\underline{1} \oplus 1)(\underline{1} \oplus 0), \end{aligned} \quad (13)$$

where  $\oplus$  represents the XOR operation. Eq. (13) may be written in a more compact manner as

$$[\tilde{u}_2 \tilde{u}_4] = [u_2 u_4] \boxplus [u_1 u_3], \quad (14)$$

hence we have

$$[u_2 u_4] = [u_1 u_3] \boxplus [\tilde{u}_2 \tilde{u}_4], \quad (15)$$

<sup>6</sup>As shown in [13], the natural-mapping and the Gray-mapping are identical for 4-QAM.

TABLE I  
GENERATING UNITS OF 16QAM USING GRAY MAPPING

Index	Generating Unit	Bit Sequence	Symbol	Quadrant	Index	Generating Unit	Bit Sequence	Symbol	Quadrant
1	2 1 2 <i>i i</i>	-1 -1 -1 -1	-3 -3 <i>i</i>	III	9	2 -1 2 <i>i i</i>	+1 +1 -1 -1	1 -3 <i>i</i>	IV
2	2 1 2 <i>i i</i>	-1 -1 -1 +1	-3 - <i>i</i>		10	2 -1 2 <i>i i</i>	+1 +1 -1 +1	1 - <i>i</i>	
3	2 1 2 <i>i -i</i>	-1 -1 +1 +1	-3 + <i>i</i>		11	2 -1 2 <i>i -i</i>	+1 +1 +1 +1	1 + <i>i</i>	I
4	2 1 2 <i>i -i</i>	-1 -1 +1 -1	-3 +3 <i>i</i>		12	2 -1 2 <i>i -i</i>	+1 +1 +1 -1	1 +3 <i>i</i>	
5	2 1 2 <i>i -i</i>	-1 +1 +1 -1	-1 +3 <i>i</i>	II	13	2 -1 2 <i>i -i</i>	+1 -1 +1 -1	3 +3 <i>i</i>	
6	2 1 2 <i>i -i</i>	-1 +1 +1 +1	-1 + <i>i</i>		14	2 -1 2 <i>i -i</i>	+1 -1 +1 +1	3 + <i>i</i>	
7	2 1 2 <i>i i</i>	-1 +1 -1 +1	-1 - <i>i</i>		15	2 -1 2 <i>i i</i>	+1 -1 -1 +1	3 - <i>i</i>	IV
8	2 1 2 <i>i i</i>	-1 +1 -1 -1	-1 -3 <i>i</i>		16	2 -1 2 <i>i i</i>	+1 -1 -1 -1	3 -3 <i>i</i>	

where  $\boxplus$  is the element-wise XOR operator. It may be readily shown that (14) and (15) also hold for the other three quadrants.

#### IV. THE PROPOSED DVA-SDPR DETECTOR

##### A. DVA-SDPR Formulation

Based on (12), the system model (1) can be rewritten as

$$\mathbf{y} = [\mathbf{h}_1, \mathbf{h}_2, \dots, \mathbf{h}_{N_T}] \begin{bmatrix} 2s_1^{(1)} + s_1^{(2)} \\ 2s_2^{(1)} + s_2^{(2)} \\ \vdots \\ 2s_{N_T}^{(1)} + s_{N_T}^{(2)} \end{bmatrix} + \mathbf{n} = [2\mathbf{H} \quad \mathbf{H}]\mathbf{x} + \mathbf{n}, \quad (16)$$

where  $\mathbf{h}_j$  is the  $j$ th column of  $\mathbf{H}$ ,  $\mathbf{x} = [s_1^{(1)}, s_2^{(1)}, \dots, s_{N_T}^{(1)}, s_1^{(2)}, s_2^{(2)}, \dots, s_{N_T}^{(2)}]^T$  with each element being a standard 4-QAM symbol. At this stage, (16) may be regarded as a virtual 4-QAM aided  $(2N_T \times N_R)$ -element MIMO system<sup>7</sup>.

According to the modulation matrix of 4-QAM given in [13], (16) can be further reformulated as

$$\mathbf{y} = [2\mathbf{H} \quad \mathbf{H}]\mathbf{W}\mathbf{p} + \mathbf{n} = \mathbf{G}\mathbf{p} + \mathbf{n}, \quad (17)$$

where  $\mathbf{G}$  is the “composite channel matrix”,  $\mathbf{p} \in \{-1, +1\}^{4N_T}$ , and

$$\mathbf{W} = \begin{bmatrix} 1 & i & 0 & 0 & \cdots & 0 & 0 \\ 0 & 0 & 1 & i & \cdots & 0 & 0 \\ 0 & 0 & 0 & 0 & \ddots & 0 & 0 \\ 0 & 0 & 0 & 0 & \cdots & 1 & i \end{bmatrix}_{2N_T \times 4N_T} \quad (18)$$

is the modulation matrix of 4-QAM for both natural-mapping and Gray-mapping. Hence the original Gray-coded 16-QAM  $(N_T \times N_R)$ -element MIMO channel has been converted to a virtual  $(4N_T \times N_R)$ -element MIMO channel relying on binary signaling.

The original ML detection related constrained discrete least-squares optimization problem of (2) may be shown to be equivalent to the following BQP problem [5]

$$\begin{aligned} \min \quad & \mathbf{p}^T \mathbf{G}^H \mathbf{G} \mathbf{p} - 2\mathbf{y}^H \mathbf{G} \mathbf{p} \\ \text{s.t. } & \mathbf{p} \in \{-1, +1\}^{4N_T}, \end{aligned} \quad (19)$$

which is difficult to solve due to the non-convex constraints of  $p_i^2 = 1$ .

In order to cast the objective function of (19) into a homogeneous quadratic form, we introduce a redundant scalar  $t \in \{+1, -1\}$ . Since

<sup>7</sup>This virtual MIMO system is not exactly equivalent to a real  $(2N_T \times N_R)$ -element MIMO system, because the left half and the right half of the virtual channel matrix  $[2\mathbf{H} \quad \mathbf{H}]$  are fully correlated, both relying on  $\mathbf{H}$ .

$t\mathbf{p} \in \{+1, -1\}^{4N_T}$  for any  $\mathbf{p} \in \{-1, +1\}^{4N_T}$ , (19) may also be formulated as

$$\begin{aligned} \min \quad & \left[ \begin{bmatrix} \mathbf{p}^T & t \end{bmatrix} \Re \{\mathbf{Q}_c\} \begin{bmatrix} \mathbf{p}^T & t \end{bmatrix}^T \right] \\ \text{s.t. } & \left[ \begin{bmatrix} \mathbf{p}^T & t \end{bmatrix} \right] \in \{+1, -1\}^{4N_T+1}, \end{aligned} \quad (20)$$

where  $\Re \{\mathbf{Q}_c\}$  represents the real part of the Hermitian matrix

$$\mathbf{Q}_c \triangleq \begin{bmatrix} \mathbf{G}^H \mathbf{G} & -\mathbf{G}^H \mathbf{y} \\ -\mathbf{y}^H \mathbf{G} & 0 \end{bmatrix}. \quad (21)$$

Upon defining  $\mathbf{x} \triangleq [\mathbf{p}^T \quad t]^T$  and  $\mathbf{Q} \triangleq \Re \{\mathbf{Q}_c\}$ , (20) may be written in the following homogeneous quadratic form

$$\begin{aligned} \min \quad & \mathbf{x}^T \mathbf{Q} \mathbf{x} \\ \text{s.t. } & \mathbf{x} \in \{+1, -1\}^{4N_T+1}, \end{aligned} \quad (22)$$

where  $\mathbf{Q}$  is a symmetric matrix. Since we have  $\mathbf{x}^T \mathbf{Q} \mathbf{x} = \text{Trace}(\mathbf{Q} \mathbf{x} \mathbf{x}^T) = \text{Trace}(\mathbf{x} \mathbf{x}^T \mathbf{Q})$ , the problem of (22) may be equivalently rewritten as

$$\begin{aligned} \min \quad & \text{Trace}(\mathbf{X} \mathbf{Q}) \\ \text{s.t. } & \mathbf{X} \succeq 0, \\ & \text{rank}(\mathbf{X}) = 1, \\ & \text{diag}(\mathbf{X}) = \mathbf{e}_{4N_T+1}, \end{aligned} \quad (23)$$

where  $\mathbf{X} = \mathbf{x} \mathbf{x}^T$ ,  $\mathbf{x} \in \{+1, -1\}^{4N_T+1}$ ,  $\text{diag}(\mathbf{X})$  is the vector composed by the diagonal elements of  $\mathbf{X}$ ,  $\mathbf{e}_{4N_T+1}$  is the “all-ones” vector of length  $4N_T+1$ , and  $\mathbf{X} \succeq 0$  indicates that  $\mathbf{X}$  is a symmetric and positive semidefinite (PSD) matrix. Due to the constraint of  $\text{rank}(\mathbf{X}) = 1$ , the problem (23) is non-convex, hence it is difficult to solve. However, by dropping the constraint of  $\text{rank}(\mathbf{X}) = 1$ , the problem of (23) may be *relaxed* to

$$\begin{aligned} \min \quad & \text{Trace}(\mathbf{X} \mathbf{Q}) \\ \text{s.t. } & \mathbf{X} \succeq 0, \\ & \text{diag}(\mathbf{X}) = \mathbf{e}_{4N_T+1}. \end{aligned} \quad (24)$$

The problem of (24) is known as an instance of semidefinite programming (SDP) [4], which constitutes a more general class of optimization techniques than linear programming<sup>8</sup>. Additionally, since SDP is a subclass of convex optimization, it does not suffer from getting trapped in local minima<sup>9</sup>.

##### B. DVA-SDPR Solving Method

The SDP problem of (24) is solved using the efficient primal-dual interior-point algorithm of [14], which guarantees a polynomial-

<sup>8</sup>Several standard optimization problems, such as linear and quadratic programming can be unified under the framework of SDP [4].

<sup>9</sup>This does not mean that the SDPR detector is always capable of achieving the optimal ML performance, because the problem of (24) is a relaxed version of the original ML optimization problem of (19).

time<sup>10</sup> worst-case complexity. The Lagrange dual problem associated with (24) is formulated as

$$\begin{aligned} \max & \quad \mathbf{e}_{4N_T+1}^T \mathbf{v} \\ \text{s. t. } & \quad \mathbf{Z} = \mathbf{Q} - \text{Diag}(\mathbf{v}) \succeq 0, \end{aligned} \quad (25)$$

where  $\text{Diag}(\mathbf{v})$  represents a diagonal matrix with its diagonal elements being  $\mathbf{v}$ .

When the objective function values of the primal problem (24) and of its dual problem (25) satisfy

$$\text{Trace}(\mathbf{X}\mathbf{Q}) - \mathbf{e}_{4N_T+1}^T \mathbf{v} \leq \max \left[ 1.0, \text{abs} \left( \mathbf{e}_{4N_T+1}^T \mathbf{v} \right) \right] \times \epsilon, \quad (26)$$

the primal-dual interior-point algorithm is deemed to have converged, where the so-called convergence tolerance  $\epsilon = 10^{-k}$  associated with an integer  $k \geq 1$ , controls the accuracy of convergence.

After obtaining the solution matrix  $\mathbf{X}^*$  of the problem (24), the solution vector  $\mathbf{p}^*$  of the problem (19) may be derived with the aid of several post-processing techniques [8], among which the simplest one is

$$\mathbf{p}^* = \text{sgn}(\mathbf{X}_{1:4N_T, 4N_T+1}), \quad (27)$$

with  $\mathbf{X}_{1:4N_T, 4N_T+1}$  denoting the first  $4N_T$  elements of the last column of  $\mathbf{X}$ . As shown by (12), the vector  $\hat{\mathbf{u}} = (\mathbf{p}^* + \mathbf{e}_{4N_T})/2$  contains half of the original information bit vector  $\mathbf{u}^*$ . The remaining half of  $\mathbf{u}^*$  may be obtained from  $\hat{\mathbf{u}}$  with the aid of the element-wise XOR operations of (15).

### C. Performance Refinement Using Bit-Flipping

The proposed DVA-SDPR detector exhibits an unequal error protection for the bits in different positions of a single 16-QAM symbol<sup>11</sup>. This may be explained with the aid of (12), where the bits  $u_1$  and  $u_3$  are mapped to a 4-QAM constellation having a doubled amplitude. Inspired by this observation, corresponding to (17), each time we may flip the sign of the  $i$ th bit  $p_i^*$  of  $\mathbf{p}^*$ ,  $i = 2N_T + 1, \dots, 4N_T$ , to obtain a modified solution vector  $\tilde{\mathbf{p}}_i^*$ . There will be a total of  $2N_T$  modified solution vectors. The final solution vector is chosen as the one, which minimizes  $\|\mathbf{y} - \mathbf{G}\mathbf{p}\|_2^2$ , when considering  $\mathbf{p}^*$  and  $\tilde{\mathbf{p}}_i^*$ .

### D. Complexity Analysis

The SDP problem of (24) involves a matrix variable  $\mathbf{X}$  of size  $(4N_T + 1) \times (4N_T + 1)$ , which entails a computational complexity of  $O[(4N_T + 1)^{3.5}]$ , when employing the primal-dual interior-point algorithm of [14]. The complexity of the  $\text{sgn}(\cdot)$  operations of (27), the XOR operations of (15) and the operations of the bit-flipping as well as the  $2N_T$  Euclidean distance computations do not affect the complexity order. Hence the overall complexity of recovering the original information bit vector is on the order of  $O[(4N_T + 1)^{3.5}]$ .

## V. SIMULATION RESULTS

In this section, we characterize the achievable performance versus the computational complexity imposed by the proposed DVA-SDPR MIMO detector for the classic Gray-mapping aided 16-QAM modulation using Monte Carlo (MC) simulations. The average SNR per receive antenna is defined as

$$\text{SNR} \triangleq 10 \log_{10} \left( E \left\{ \|\mathbf{H}\mathbf{s}\|^2 / N_R \right\} / 2\sigma^2 \right) = 10 \log_{10} \left( N_T / 2\sigma^2 \right). \quad (28)$$

<sup>10</sup>The complexity increases as a polynomial function of the problem size, which is determined by the number of rows (or columns) of the symmetric cost matrix  $\mathbf{Q}$  of (24) in the considered context. Here  $\mathbf{Q}$  is the input argument of the primal-dual interior-point algorithm of [14].

<sup>11</sup>Observe in Fig. 2 of Section V, the first and the third bits (resp. the second and the fourth bits), namely  $u_1$  and  $u_3$  (resp.  $u_2$  and  $u_4$ ) in a single 16-QAM symbol exhibit an identical BER performance, which is better (resp. worse) than the overall BER performance. Due to space limitation, Fig. 2 will not be explained again in Section V.

The computational complexity is quantified in terms of the number of equivalent additions, denoted as  $N_{\text{add}}$ , required for decoding a single transmitted MIMO symbol vector. More explicitly, we have  $N_{\text{add}} \triangleq E\{T_{\text{tot}}\}/E\{T_{\text{add}}\}$ , where  $T_{\text{tot}}$  is the average time required for decoding a MIMO symbol vector, while  $T_{\text{add}}$  is the average computation-time per addition operation. Compared to the “execution-time” metric used in [9], this complexity metric has the advantage of being independent of different simulation platforms<sup>12</sup>. An  $(8 \times 8)$ -element flat Rayleigh fading MIMO channel is considered, where the MIMO channel-matrix entries are chosen as independent and identically distributed (i.i.d.), zero mean, unit-variance complex-valued Gaussian random variables. Hence the system’s total throughput is  $8 \times 4 = 32$  bits/MIMO symbol vector. A new realization of the channel matrix is drawn for each transmitted symbol vector. Each element of the noise vector  $\mathbf{n}$  is i.i.d. and  $\mathcal{CN}(0, 2\sigma^2)$ . Since it has been shown that the SDPR detectors of [8], [9] and [11] are equivalent in performance, below we will consider the index-bit-based VA-SDPR (IVA-SDPR) of [11] as one of the benchmarkers.

In Fig. 3, we contrasted the BER performance of the proposed DVA-SDPR (with or without bit-flipping) to that of these benchmarkers, namely to that of the IVA-SDPR of [11], of the minimum-mean-square-error-ordered-successive-interference-cancelation (MMSE-OSIC), and of the SD relying on an adaptive sphere radius for the sake of achieving the exact ML performance<sup>13</sup>. Observe in Fig. 3 that the proposed DVA-SDPR detector operating without bit-flipping achieves a BER performance identical to that of the IVA-SDPR benchmark. By contrast, the bit-flipping aided DVA-SDPR outperforms the IVA-SDPR by about 2dB at  $\text{BER} = 10^{-3}$  and  $\text{BER} = 10^{-4}$ . As expected, all the SDPR detectors considered exhibit a superior BER performance compared to the MMSE-OSIC detector. However, unlike in the BPSK scenario, where the SDPR detector achieves the maximum attainable diversity [6], in the 16-QAM scenario considered, the DVA-SDPR and IVA-SDPR detectors suffer from a considerable performance degradation in the high SNR region compared to the SD. This indicates that the SDPR detectors considered might not be able to achieve full diversity for the Gray-coded 16-QAM aided  $(8 \times 8)$ -element MIMO fading channel.

In Fig. 4, we compared the complexity of the detectors considered in Fig. 3. It is readily seen that the SD imposed a significantly higher computational complexity in the low-SNR region than in the high-SNR region, which is consistent with the theoretical results of [3]. By comparison, the computational complexities of both the proposed DVA-SDPR detectors operating with and without bit-flipping as well as the IVA-SDPR detector are near-constant. More specifically, the DVA-SDPR dispensing with bit-flipping has a slightly lower complexity than the IVA-SDPR benchmark, since the IVA-SDPR detector requires the computation of Eq. (4) plus the computation of 16 Euclidean distances for deciding upon each transmitted 16-QAM symbol, before proceeding to the information-bit decisions. On the other hand, the DVA-SDPR using bit-flipping imposes a computational complexity near-identical to that of the IVA-SDPR. Furthermore, the complexity of both the IVA-SDPR and the DVA-SDPR detectors is considerably lower than that of the SD detector, but still higher than that of the MMSE-OSIC detector.

To the best of our knowledge, in the uncoded Gray-mapping aided 16-QAM  $(8 \times 8)$ -element MIMO scenario considered, the DVA-SDPR using bit-flipping achieves the best BER performance result among the known SDPR-aided MIMO detectors, while still maintaining a polynomially increasing worst-case complexity order of  $O[(4N_T + 1)^{3.5}]$ . Additionally, since the proposed DVA-SDPR detector directly generates the information-bit decisions without

<sup>12</sup>For a given algorithm, both  $T_{\text{tot}}$  and  $T_{\text{add}}$  should be measured in the same simulation platform, where  $T_{\text{add}}$  serves as a normalizing unit.

<sup>13</sup>This SD is based on the classic SD of [1], and the minimum sphere radius was set to 2.

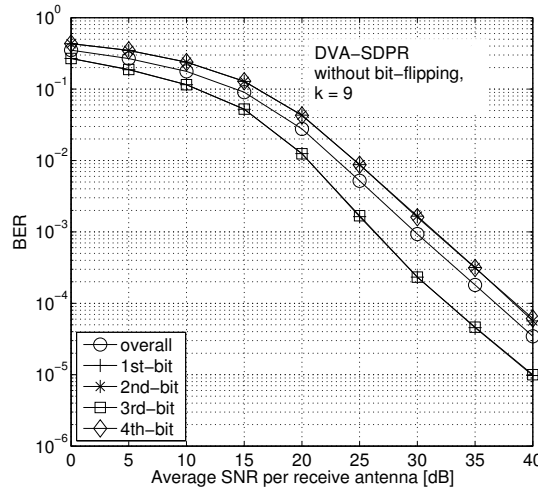


Fig. 2. Unequal error protection of the DVA-SDPR for Gray-coded 16-QAM aided  $(8 \times 8)$ -element MIMO over uncorrelated flat Rayleigh fading channels, with the convergence tolerance  $\epsilon = 10^{-9}$ .

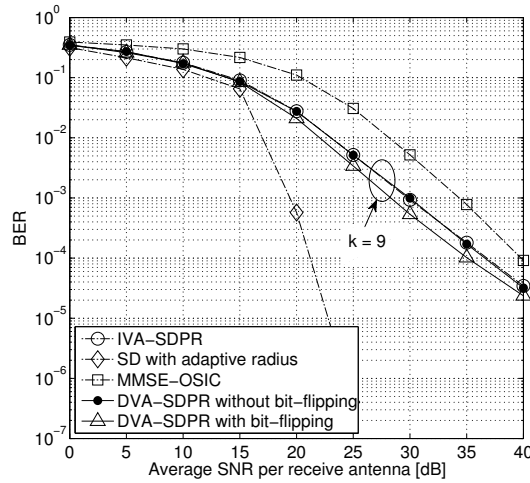


Fig. 3. Performance comparison of the DVA-SDPR, IVA-SDPR, SD and MMSE-OSIC detectors for 16-QAM aided  $(8 \times 8)$ -element MIMO over uncorrelated flat Rayleigh fading channels.

first making symbol decisions, it may reduce the hardware cost in practical applications. In general, the DVA-SDPR, the IVA-SDPR and the MMSE-OSIC detectors may serve as efficient alternatives for the SD in the low-SNR region, say below about 15dB in the context considered. The SDPR detectors achieve full-diversity in a BPSK scenario, hence an interesting problem for future research is to conceive efficient SDPR detectors that can approach the ML performance for high-order QAM.

## VI. CONCLUSIONS

In contrast to the existing IVA-SDPR detector, the proposed DVA-SDPR detector bypasses symbol-decisions and directly generates the information bits of classic Gray-mapping aided 16-QAM by employing a simple linear matrix representation (LMR) of 4-QAM. In principle the proposed method may be extended to general high-order rectangular QAM constellations. Based on this contribution, the MIMO detector and constellation demapper modules of high-order rectangular QAM using either linear natural mapping or nonlinear Gray mapping may be replaced by a single DVA-SDPR detector, which performs detection and demapping jointly. Furthermore, when

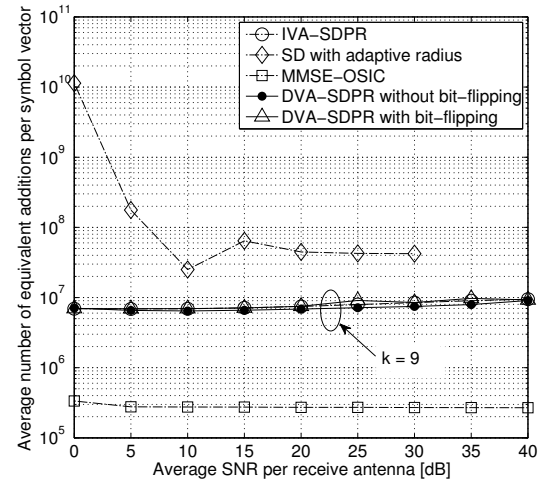


Fig. 4. Complexity comparison of the DVA-SDPR, IVA-SDPR, SD and MMSE-OSIC detectors for 16-QAM aided  $(8 \times 8)$ -element MIMO over uncorrelated flat Rayleigh fading channels.

combined with low-complexity bit-flipping based “hill climbing”, the proposed DVA-SDPR detector achieves the best BER performance among the known SDPR-based detectors in the context considered, while still maintaining a polynomial-time worst-case complexity order of  $O[(4N_T + 1)^{3.5}]$ .

## REFERENCES

- [1] E. Viterbo and J. Boutros, “A universal lattice code decoder for fading channels,” *IEEE Transactions on Information Theory*, vol. 45, no. 7, pp. 1639–1642, Jul. 1999.
- [2] L. Hanzo, Y. Akhtman, L. Wang, and M. Jiang, *MIMO-OFDM for LTE, WiFi and WiMAX: Coherent versus Non-Coherent and Cooperative Turbo-Transceivers*. Chichester, UK: Wiley, 2010.
- [3] J. Jaldén and B. Ottersten, “On the complexity of sphere decoding in digital communications,” *IEEE Transactions on Signal Processing*, vol. 53, no. 4, pp. 1474–1484, Apr. 2005.
- [4] L. Vandenberghe and S. Boyd, “Semidefinite programming,” *SIAM Review*, vol. 38, no. 1, pp. 49–95, Mar. 1996.
- [5] S. Boyd and L. Vandenberghe, *Convex Optimization*. New York, USA: Cambridge University Press, 2004.
- [6] J. Jaldén and B. Ottersten, “The diversity order of the semidefinite relaxation detector,” *IEEE Transactions on Information Theory*, vol. 54, no. 4, pp. 1406–1422, Apr. 2008.
- [7] W.-K. Ma, P.-C. Ching, and Z. Ding, “Semidefinite relaxation based multiuser detection for M-ary PSK multiuser systems,” *IEEE Transactions on Signal Processing*, vol. 52, no. 10, pp. 2862–2872, Oct. 2004.
- [8] A. Wiesel, Y. C. Eldar, and S. S. Shitz, “Semidefinite relaxation for detection of 16-QAM signaling in MIMO channels,” *IEEE Signal Processing Letters*, vol. 12, no. 9, pp. 653–656, Sep. 2005.
- [9] N. D. Sidiropoulos and Z.-Q. Luo, “A semidefinite relaxation approach to MIMO detection for high-order QAM constellations,” *IEEE Signal Processing Letters*, vol. 13, no. 9, pp. 525–528, Sep. 2006.
- [10] A. Mobasher, M. Taherzadeh, R. Sotirov, and A. K. Khandani, “A near-maximum-likelihood decoding algorithm for MIMO systems based on semi-definite programming,” *IEEE Transactions on Information Theory*, vol. 53, no. 11, pp. 3869–3886, Nov. 2007.
- [11] Z. Mao, X. Wang, and X. Wang, “Semidefinite programming relaxation approach for multiuser detection of QAM signals,” *IEEE Transactions on Wireless Communications*, vol. 6, no. 12, pp. 4275–4279, Dec. 2007.
- [12] W.-K. Ma, C.-C. Su, J. Jaldén, T.-H. Chang, and C.-Y. Chi, “The equivalence of semidefinite relaxation MIMO detectors for higher-order QAM,” *IEEE Journal of Selected Topics in Signal Processing*, vol. 3, no. 6, pp. 1038–1052, Dec. 2009.
- [13] S. Yang, T. Lv, R. Maundier, and L. Hanzo, “Unified bit-based probabilistic data association aided MIMO detection for high-order QAM constellations,” *IEEE Transactions on Vehicular Technology*, vol. 60, no. 3, pp. 981–991, Mar. 2011.
- [14] C. Helmberg, F. Rendl, R. J. Vanderbei, and H. Wolkowicz, “An interior-point method for semidefinite programming,” *SIAM Journal on Optimization*, vol. 6, pp. 342–361, 1996.